Neural Network-based Load-Frequency Control in Power Grids

Prabin Mali and Sumit Paudyal Florida International University, USA Emails: {pmali004, spaudyal}@fiu.edu

Abstract—Any change in load or trip of generator causes power mismatch in the system which is initially compensated by the kinetic energy stored in the form of inertia and then by the governor control actions. In order to keep the frequency at nominal value and also to keep the tieline flow at the scheduled value, Load Frequency Control is employed. As the controller needs to be robust, we proposed a Load Frequency Controller based on LSTM Neural Network. To validate the performance of the proposed controller, it is compared with traditional integral controller with various disturbance like increment of load, decrement of load, and removal of generating units. The results show that the proposed LSTM controller is able to capture the details of the dynamics of the traditional integral controller and can be used in place of the traditional controller in single area as well as two-area power systems.

Index Terms—Automatic Generation Control, Load Frequency Control, Long Short Term Memory (LSTM), Integral Controller

I. Introduction

In power grids, when a generator is tripped or a load is added to the system, the power mismatch occurs and is initially compensated by an extraction of the kinetic energy from the inertial storage of system that causes decline in system frequency. When the frequency decreases, the power consumed by loads decreases. For large system, in case of small disturbance, this reduction in loads may balance the change in powers due to addition of load or tripping of generator. If the frequency deviation is beyond the deadband, the output will be increased by the governor action and a new equilibrium is achieved [1]. Although the governor action can lead an equilibrium state, large deviation in frequency from the nominal value may lead to undesirable effects [2]. A large deviation in frequency can degrade performance of load, damage connected load, can interfere with system protection scheme that ultimately leads the power system to be unstable with possibility of such as blackouts or cascading failures [3][4]. Therefore, in order to keep the frequency at the nominal value, a control system is essential. This control system, also known as Automatic Generation Control (AGC) or Load Frequency Control (LFC) has two primary objectives, i.e., maintaining the frequency at the nominal value, and maintaining power interchanges with neighboring control areas at the scheduled values. To fulfill these objectives, sum of weighted deviation of frequency and power interchanges, also known as Area Control Error (ACE) is calculated which is fed to a controller which tries to make the ACE zero by changing the reference input to the governors of participating generators.

The AGC problem has been investigated rigorously in the past many decades including the usage of machine learning tools. In [5], [6], [7], Feed Forward Neural Networks were used to in place of traditional controllers for the AGC. In [8]. hierarchical Neural Network (NN) is used as single NN is not sufficient to replace the traditional controllers. In [9], [10], Artificial Neural Network (ANN) is used in conjunction with Fuzzy logic. All of the above mentioned work uses the Feed-Forward Neural Network (FFNN), which has simple inputoutput relationship and are not able to represent the behavior of the controllers for the transient response of power system as FFNNs do not consider historical input and output data, and solely depend on the present value of the inputs. To overcome this problem, a special type of Neural Network, called Recurrent Neural Network (RNN), more specifically with Long Short Term Memory (LSTM) unit, can be used as a controller which not only considers the present values of the inputs but also the past values of the inputs and outputs.

This paper presents a Load Frequency Controller based on the LSTM Neural Network that is able to regulate the frequency of the power system and also regulate the tieline power flows between two areas of the system.

The rest of the paper is organized as following. Section II presents the dynamic models of synchronous generators, governors, Load Frequency Controller, and the LSTM Neural Network. Section III presents the test system used in simulation and the setup. Controller Design and Model Validation are discussed in Section IV. Conclusion and future works are discussed in Section V.

II. MATHEMATICAL MODELING

A. Power System Dynamics

We model a power system using a classical representation of synchronous generators and non-linear power flow. The dynamic behavior of synchronous generators can be represented using the Swing Equation as (1) and (2), where δ_i represents the rotor angle of synchronous generator i and is considered equal to terminal voltage angle; ω_i represents speed of generator; \mathcal{P}_i^M and \mathcal{P}_i^G are mechanical and generator output power of generator; D_i is the damping coefficient, and H_i is inertia constant. Also, $\mathcal{N}^{\mathcal{G}}$ is the set of generators.

$$\frac{d\delta_i}{dt} = \omega_i - \omega_0, \forall i \in \mathcal{N}^G$$
 (1)

$$\frac{d\omega_i}{dt} = \frac{1}{2H_i} \left(\mathcal{P}_i^M - \mathcal{P}_i^G - D_i \Delta \omega_i \right), \forall i \in \mathcal{N}^G$$
 (2)

The power flow can be represented by non-linear equations (3) and (4). These equations give the net active power $(\mathcal{P}_i^G - \mathcal{P}_i^L)$ and reactive power $(\mathcal{Q}_i^G - \mathcal{Q}_i^L)$ injected to the bus i. Here, \mathcal{V}_i and \mathcal{V}_k represent voltage at bus i and k respectively; and δ_k represent voltage angles at bus i and k respectively; and \mathcal{V}_{ik} and θ_{ik} represent magnitude and angle of admittance between buses i and k. Also, \mathcal{N} is the set of all the buses.

$$\mathcal{P}_{i}^{G} - \mathcal{P}_{i}^{L} = \mathcal{V}_{i} \sum_{k \in \mathcal{N}} \mathcal{V}_{k} \mathcal{Y}_{ik} cos(\theta_{ik} + \delta_{i} - \delta_{k}), \forall i, k \in \mathcal{N}$$
(3

$$Q_i^G - Q_i^L = -\mathcal{V}_i \sum_{k \in \mathcal{N}} \mathcal{V}_k \mathcal{Y}_{ik} sin(\theta_{ik} + \delta_i - \delta_k), \forall i, k \in \mathcal{N}$$
(4)

The governor model TGOV1, which is the simplified representation of the steam governor, is considered and can be represented by (5), where \mathcal{P}_i^R and \mathcal{P}_i^V are the reference power and output power of governor $i; T_i$ is the time constant of governor and $1/R_i$ is the speed regulation or the droop characteristics of the governor. Also, \mathcal{N}^{GV} is the set of governors.

$$\mathcal{P}_{i}^{V} = \frac{1}{T_{i}} \int \left(\mathcal{P}_{i}^{R} - \frac{\Delta \omega_{i}}{R_{i}} - \mathcal{P}_{i}^{V} \right) dt, \forall i \in \mathcal{N}^{GV}$$
 (5)

B. Load Frequency Control

1) Load Frequency Control of Single Area Power System: Fig. 1 shows the single area power system represented by equivalent load and single synchronous generator with corresponding turbine and governor. Here, B is the frequency bias factor which is given as the sum of frequency dependent load change (D) and speed regulation (1/R). The controller considered in this case is the integral controller and is represented by (6) and (7), where \mathcal{E} is the error, \mathcal{K}^I is the gain of the controller, and \mathcal{P}^R is the reference power (output of controller) which is fed to the governor.

$$\mathcal{E} = -B\,\Delta\omega\tag{6}$$

$$\mathcal{P}^R = \mathcal{K}^I \int \mathcal{E}dt \tag{7}$$

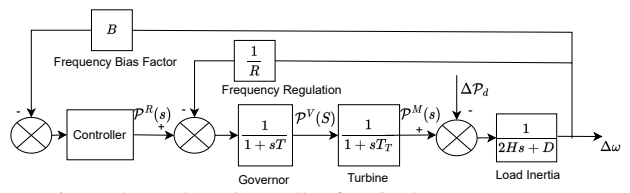


Fig. 1: Secondary Controller for single area power system.

2) Load Frequency Control of Two Area Interconnected Power System: Fig. 2 shows the two area interconnected power system of non-reheat thermal plant which is widely used for the analysis of load frequency control system. In Fig. 2, ACE_1 and ACE_2 are the area control errors; and B_1 and B_2 are frequency bias factors for area 1 and area 2, respectively. $\Delta \mathcal{P}_{12}^{tie}$ is the difference between actual power flow and scheduled power flow in tieline from area 1 to area 2. The controllers considered in this case are integral controllers and are represented by generalized equations (8) and (9), where \mathcal{P}_{jk}^{tie} and \mathcal{P}_{jk}^{sch} are respectively current and scheduled tie-line power flows from area j to area k; and ACE_j , $\Delta\omega_j$, B_j , \mathcal{K}_j^I and \mathcal{P}_j^R are respectively Area Control Error (ACE), frequency deviation, frequency bias factor, integral constant, and output of the controller of area j.

$$ACE_j = (B_j)(\Delta\omega_j) + \sum_{k \in \mathcal{Z}} (\mathcal{P}_{jk}^{tie} - \mathcal{P}_{jk}^{sch})$$
 (8)

$$\mathcal{P}_j^R = \mathcal{K}_j^I \int ACE_j dt \tag{9}$$

C. LSTM Neural Network

Long Short Term Memory (LSTM) Network is a variant of Recurrent Neural Network (RNN) [11]. LSTM is capable of retrieving information from previous timestep. It can also forget and update the data in internal memory cells in each timestep. As it is a RNN, it performs better for time-series learning problems. The structure of the LSTM cell contains input gate, forget gate, and output gate. The LSTM defines and maintains the cell state to manage information flow to acquire long-term temporal functional relationships [12].

Fig. 3 shows the detailed diagram of a single LSTM unit [13]. The input gate decides what to preserve in the current memory cell state, the forget gate decides what to forget from the previous memory cell state and output gate decides what to pass as n LSTM output. LSTM memory units

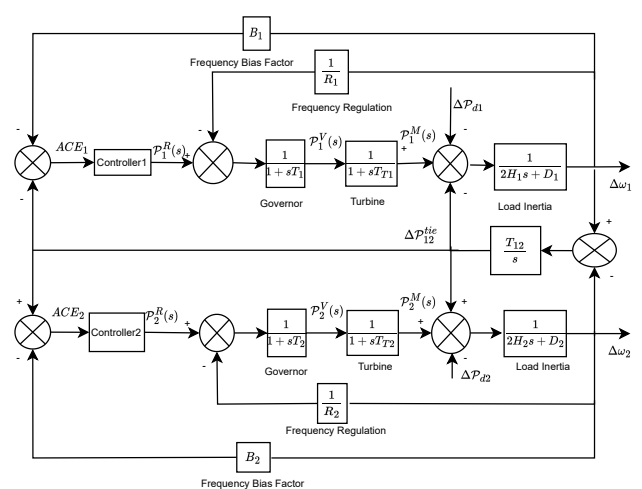


Fig. 2: Secondary Controller for two area power system.

can record sophisticated correlation patterns inside time-series data in both short and long term with the help of these gates.

Given a sequence dataset $\{x^1, x^2,, x^T\}$, where $x^t \in \mathbb{R}^m$ represents the m-dimensional vector at timestep t, the output of LSTM unit h^t is calculated based on the memory cell state C^{t-1} , intermediate output h^{t-1} and sequence input x^t .

Equation (10) represents full model of a LSTM unit where $W_{ix}, W_{fx}, W_{ox}, W_{\tilde{C}x}, W_{ih}, W_{fh}, W_{oh}$, and $W_{\tilde{C}h}$ are respective input matrices; b_i, b_f, b_o and $b_{\tilde{C}}$ are the respective bias vectors, and \odot corresponds to an element-wise multiplication operator.

$$i^{t} = \sigma(W_{ix}x^{t} + W_{ih}h^{t-1} + b_{i})$$

$$f^{t} = \sigma(W_{fx}x^{t} + W_{fh}h^{t-1} + b_{f})$$

$$o^{t} = \sigma(W_{ox}x^{t} + W_{oh}h^{t-1} + b_{o})$$

$$\tilde{C}^{t} = tanh(W_{\tilde{C}x}x^{t} + W_{\tilde{C}h}h^{t-1} + b_{\tilde{C}})$$

$$C^{t} = i^{t} \odot \tilde{C}^{t} + f^{t} \odot C^{t-1}$$

$$h^{t} = tanh(C^{t}) \odot o^{t}$$

$$(10)$$

III. SIMULATION SETUP

A. Test System

We use the well known New England IEEE 39 bus system [14] as the test system which includes 10 synchronous generators as shown in Fig. 4. It is assumed that all the generators are equipped with the governor with the frequency regulation of 5%. Also, it is assumed that the generators connected to buses 30 to 35 are capable of getting setpoints from upper level controller while generators at buses 36 to 39 have fixed setpoints. The parameters of generators and governors are provided in Table I. These values are at the base of 1000 MVA. Here, Load Damping Factor (*D*) is ignored and bus 39 is considered as a slack bus. Also, the excitation is kept constant for all the generators. The test system is developed in MATLAB/SIMULINK and solved using ePHASORsim solver.

B. Load Frequency Controller

For realizing the Load Frequency Controller two scenarios are considered.

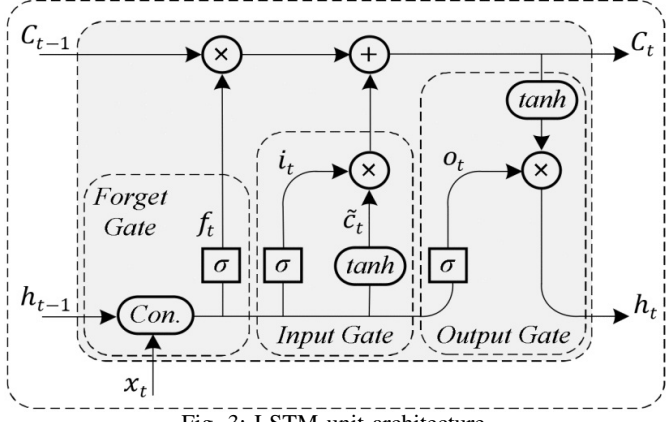


Fig. 3: LSTM unit architecture.

TABLE I: Generator and Governor Parameters

Bus No.	Generator	Governor	
	H(s)	R(p.u.)	T(s)
30	4.20	0.05	0.4
31	3.03	0.05	0.4
32	3.58	0.05	0.4
33	2.86	0.05	0.4
34	2.60	0.05	0.4
35	3.48	0.05	0.4
36	2.64	0.05	0.4
37	2.43	0.05	0.4
38	3.45	0.05	0.4
39	50.00	0.05	0.4

Scenario I: In this scenario, entire test system is considered as one area and the problem is to return the deviated frequency back to the nominal frequency after the disturbance in the system. In this case, we take change in load as the disturbance. The controller considered is an integral controller with change in frequency as input and governor reference as output. The output of the controller is fed to the governors in proportion to the nominal generation power of corresponding generators.

Scenario II: In this scenario, the test system is divided into two areas as in Fig. 4. The two areas are separated by two tielines 14-15 and 17-16. Here, the objectives are to returning the deviated frequency back to nominal frequency and the returning the deviated tieline power back to the scheduled power after the disturbance in the system. Here, each area is considered to have a separate controller and the controllers are considered to be integral type with Area Control Error (ACE) as input and the governor reference as output. Here, in this scenario, the output of the controllers are fed to the governors of corresponding area in proportion to the nominal generation power of the respective generators.

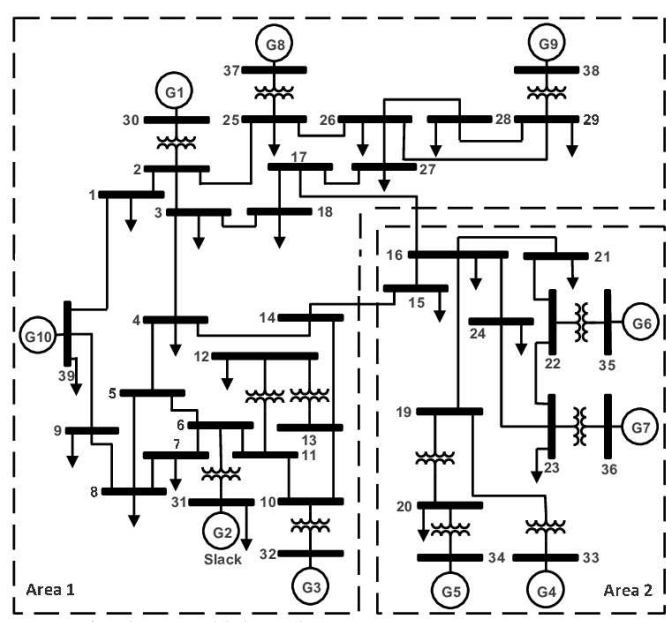


Fig. 4: IEEE 39 bus 10 generator system test system.

C. Training of Neural Network

The neural network with 5 layers is considered, the layers being one input layer, one output layer, and 3 hidden layers. The 3 hidden layers are 2 LSTM layers with 125 neurons each and one fully connected layer with 1 neuron for scenario I and 2 LSTM layers with 250 neurons each and one fully connected layer with 2 neurons for scenario II. To obtain the training data, the frequency and governor reference data are recorded by increasing and decreasing the load of each bus by 5% up to $\pm 15\%$ from the nominal value. The deep learning toolbox of MATLAB is used to train the neural network. Before feeding the Neural Network, the training data is normalized.

IV. SIMULATION STUDIES

A. Designing of Controller

The controller is designed for both the scenarios mentioned in section III.

In Scenario I, one single centralized controller is designed to control the whole area. An integral controller is chosen here as the integral controller ensures zero frequency error in steady state. The value of controller gain K^I is chosen so as to minimize the oscillation and is chosen to be 0.3. The frequency response of generators at buses 33 and 36 with and without LFC for single area test system is shown in Fig. 5. The figure shows that only after the introduction of LFC, the frequency returns to the nominal value after the disturbance is applied. The Fig. 6 shows the output power of generators at buses 33 and 36 with and without LFC. Likewise, the mechanical powers fed to generators at buses 33 and 36 with and without LFC are shown in Fig. 7.

In Scenario II, one controller for each respective areas are designed. Integral controllers are chosen in this case as well and the value of controller gains for both the controllers are chosen to be 0.3. The frequency response of generators at buses 36 and tie-line active power flow between Area 1 and Area 2 with and without LFC for the two area system are shown in Fig. 8. This shows that after the disturbance is applied in the two area system, the frequency returns back to the nominal value and the tie-line active power flow returns back to the scheduled value after the introduction of LFC.

B. Model Validation for Single Area Power system

To validate the accuracy of the trained model for single area power system, three test scenarios are considered, i.e., i) increase the load by 5%, ii) decrease the load by 5%, and iii) disconnect generator at bus 37. After training the model, the integral controller is replaced with the proposed LSTM controller. The frequency response of the test system (taking bus 33 as a candidate) and the output of the controller (governor reference) is measured for each scenario.

For scenario I, the load is increased by 5% at 5s while for scenario II, the load is decreased by 5% at 5s and the responses are recorded. Similarly, for scenario III, the generator at bus 37 is disconnected from the system at 5s and the response is recorded. The frequency response of the test system and the output of controller for Scenario I, II, and

III are shown in Fig. 9, 10, and 11, respectively. All the three graphs are plotted for the case with the integral controller and for the case after replacing with LSTM controller.

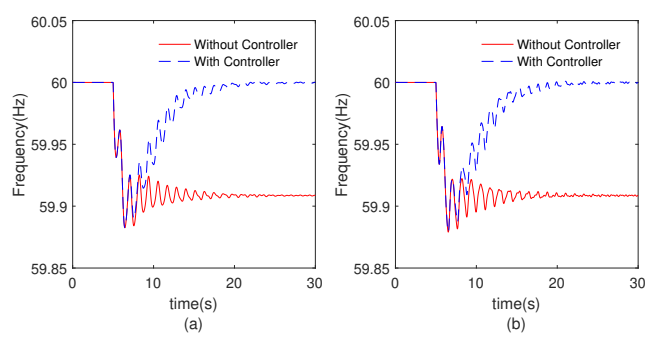


Fig. 5: Frequency Response of a) Generator at bus 33 and b) Generator at bus 35 with and without controller.

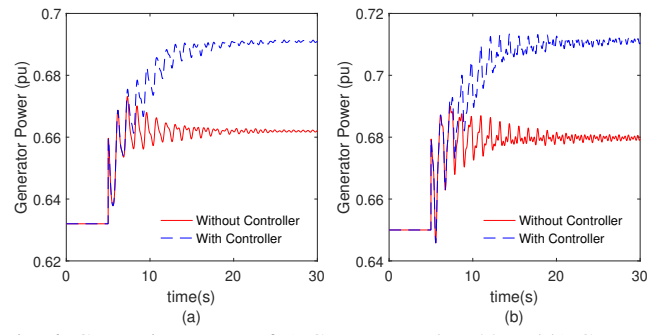


Fig. 6: Generating power of a) Generator at bus 33 and b) Generator at bus 35 with and without controller.

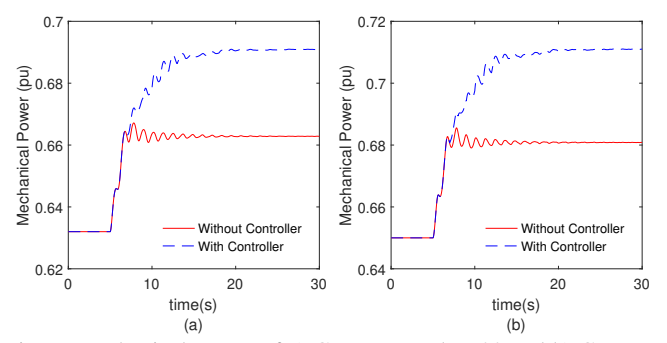


Fig. 7: Mechanical Power of a) Generator at bus 33 and b) Generator at bus 35 with and without controller.

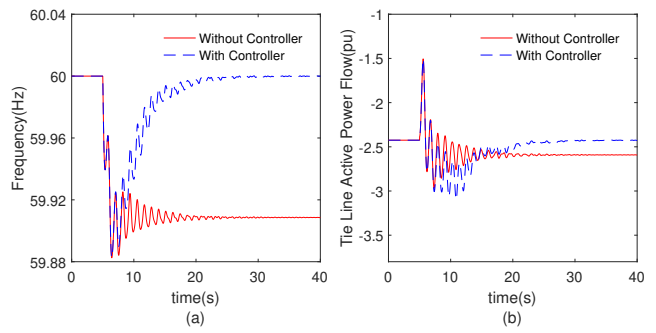


Fig. 8: a) Frequency Response of Generator at bus 33 and b) Tie-line Active Power Flow with and without controller.

Fig. 9, 10, and 11 show that the performance of LSTM controller is satisfactory for all three scenarios and can be used as a Load Frequency Controller in a single area power system.

C. Model Validation for Two Area Power system

To validate the accuracy of the trained model for two area power system, four test scenarios are considered. e.g., i) increase the load by 5%, ii) decrease the load by 5%, iii) add a 200MW load at bus 12 (area 1), and iv) add a 200MW load at bus 24 (area 2). After training the model, the integral controllers in each area are replaced with the corresponding proposed LSTM controllers. The frequency response of the

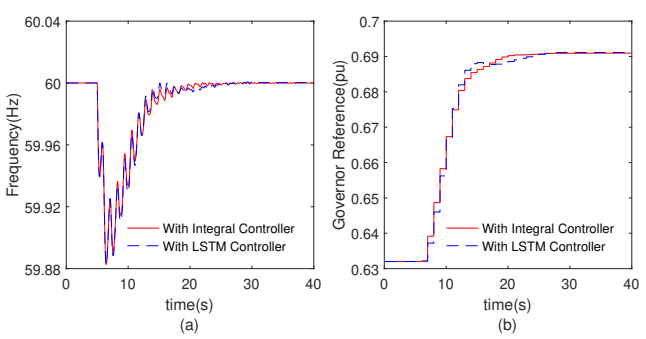


Fig. 9: a) Frequency Response of test system and b) Output of Controller (Governor Reference) subject to load increment by 5% with Integral Controller and with LSTM Controller.

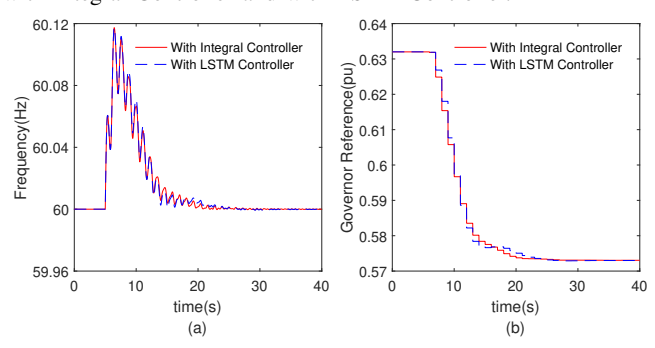


Fig. 10: (a) Frequency Response of test system and (b) Output of Controller (Governor Reference) subject to load decrement by 5% with Integral Controller and with LSTM Controller.

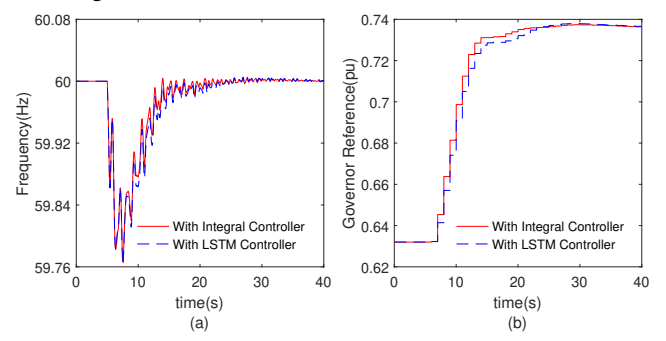


Fig. 11: (a)Frequency Response of test system and (b)output of Controller (Governor Reference) subject to shutdown of Generator at Bus 37 with Integral Controller and with LSTM Controller.

test system and the tie-line active power flow are measured for each scenario.

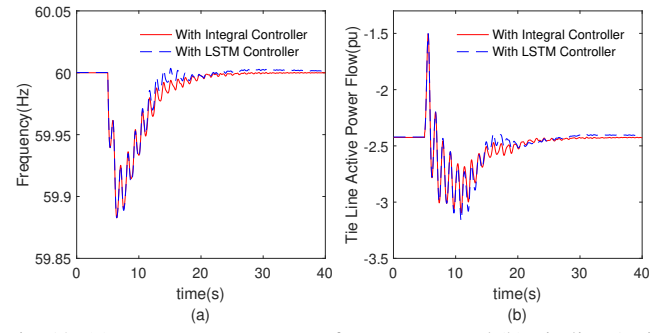


Fig. 12: (a) Frequency Response of test system and (b) Tie-line Active Power Flow subject to load increment by 5% with Integral Controller and with LSTM Controller.

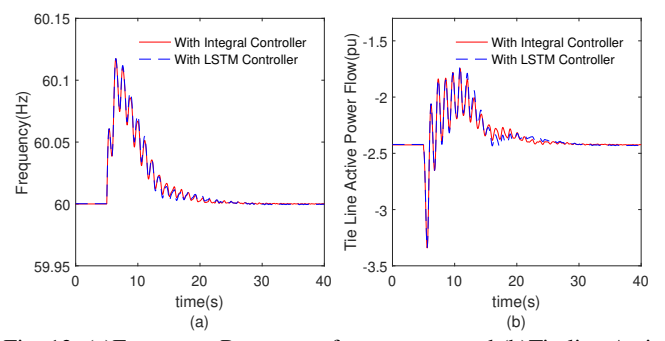


Fig. 13: (a)Frequency Response of test system and (b)Tie-line Active Power Flow subject to load decrement by 5% with Integral Controller and with LSTM Controller.

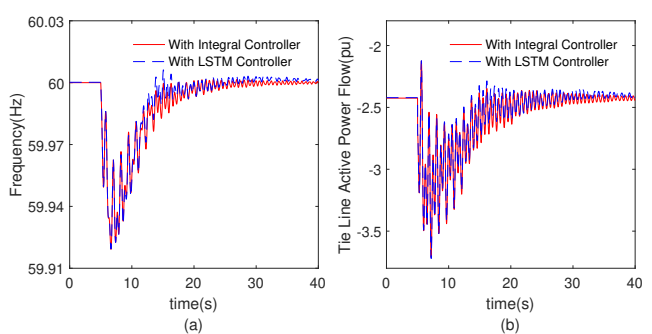


Fig. 14: (a) Frequency Response of test system and (b) Tie-line Active Power Flow subject to addition of 200MW load at bus 12 (area1) with Integral Controller and with LSTM Controller.

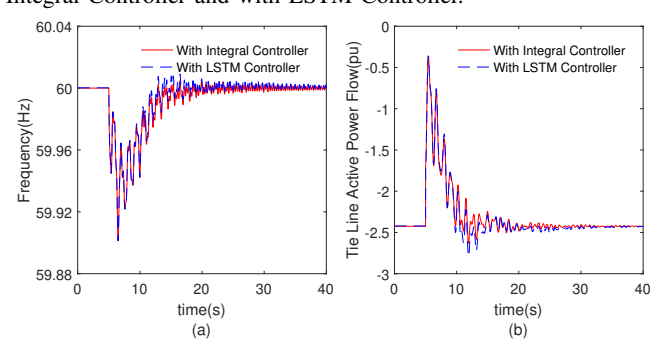


Fig. 15: (a) Frequency Response of test system and (b) Tie-line Active Power Flow subject to addition of 200MW load at bus 24 (area2) with Integral Controller and with LSTM Controller.

For scenario I, the load is increased by 5% at 5s while for scenario II, the load is decreased by 5% at 5s and the responses are recorded. For scenario III, a bulk load of 200MW is added in area 1 at bus 12 at 5s while for scenario IV, a bulk load of 200MW is added in area 2 at bus 24 at 5s and the responses are recorded. The frequency response of the test system and the Tie-line Active Power Flow for Scenario I, II, III and IV are shown in Fig. 12, 13, 14, and 15 respectively. All of these responses are plotted for the case with the integral controllers and for the case after replacing them with the LSTM controllers. It can be seen that the performance of LSTM controller is satisfactory for all the scenarios considered and can be used as a Load Frequency Controller in a two area power system which can be further expanded for multi-area power system.

V. CONCLUSION AND FUTURE WORKS

This paper presented the LSTM model of the Load Frequency Controller. We compared the performance of LSTM Neural Network with the traditional Integral Controller for various scenarios. The comparison clearly depicts that the proposed LSTM controller is able to capture the details of dynamics of the traditional integral controller and can be used in place of traditional integral controller in case of single area power system and two area power system. In future, we will model the LSTM controller for the multi-area power system.

REFERENCES

- N. Jaleeli, L. VanSlyck, D. Ewart, L. Fink, and A. Hoffmann, "Understanding automatic generation control," *IEEE Transactions on Power Systems*, vol. 7, no. 3, pp. 1106–1122, 1992.
- [2] Ibraheem, P. Kumar, and D. Kothari, "Recent philosophies of automatic generation control strategies in power systems," *IEEE Transactions on Power Systems*, vol. 20, no. 1, pp. 346–357, 2005.
- [3] H. Bevrani, Robust Power System Frequency Control. Springer International Publishing, 2014.
- [4] P. S. Kundur and O. P. Malik, Power System Stability and Control. McGraw-Hill Education, 2022.
- [5] J. Jaleel and T. Imthias Ahammed, "Simulation of artificial neural network controller for automatic generation control of hydro electric power system," in *Proc. TENCON IEEE Region 10 Conference*, pp. 1– 4, 2008.
- [6] B. P. Padhy and B. Tyagi, "Artificial neural network based multi area automatic generation control scheme for a competitive electricity market environment," in *Proc. International Conference on Power Systems*, pp. 1–6, 2009.
- [7] D. Chen and L. Wang, "Neural network based predictive automatic generation control," in *Proc. IEEE Power and Energy Society General Meeting (PESGM)*, pp. 1–5, 2016.
- [8] D. Chen and L. Wang, "Adaptive automatic generation control based on gain scheduling and neural networks," in *Proc. IEEE Power Energy Society General Meeting*, pp. 1–5, 2017.
- [9] R. Verma, S. Pal, and Sathans, "Intelligent automatic generation control of two-area hydrothermal power system using ann and fuzzy logic," in Proc. International Conference on Communication Systems and Network Technologies, pp. 552–556, 2013.
- [10] A. Ghatak, T. Pandit, S. R. Kavitha, and A. Chitra, "Modelling and analysis of automatic generation control in power systems," in *Proc. Innovations in Power and Advanced Computing Technologies (i-PACT)*, pp. 1–7, 2021.
- [11] F. Salem, Recurrent Neural Networks: From Simple to Gated Architectures. Springer International Publishing, 2022.
- [12] S. Hochreiter and J. Schmidhuber, "Long Short-Term Memory," *Neural Computation*, vol. 9, pp. 1735–1780, 11 1997.

- [13] A. S. Musleh, G. Chen, Z. Y. Dong, C. Wang, and S. Chen, "Attack detection in automatic generation control systems using LSTM-based stacked autoencoders," *IEEE Transactions on Industrial Informatics*, vol. 19, no. 1, pp. 153–165, 2023.
- [14] M. A. Pai, Energy Function Analysis for Power System Stability. Springer New York, 1989.